

UNCLASSIFIED

AD 282 925

Report of
the

ARMED SERVICES TECHNICAL INFORMATION AGENCY
ARLINGTON HALL STATION
ARLINGTON 12, VIRGINIA



UNCLASSIFIED

NOTICE: When government or other drawings, specifications or other data are used for any purpose other than in connection with a definitely related government procurement operation, the U. S. Government thereby incurs no responsibility, nor any obligation whatsoever; and the fact that the Government may have formulated, furnished, or in any way supplied the said drawings, specifications, or other data is not to be regarded by implication or otherwise in any manner licensing the holder or any other person or corporation, or conveying any rights or permission to manufacture, use or sell any patented invention that may in any way be related thereto.

62-4-5

282 925

CATALOGED AT ASTIA

282925

AD NO. _____

THE UNIVERSITY OF CONNECTICUT

SCHOOL OF ENGINEERING

TECHNICAL REPORT NO. 1

THE SHOCK WAVE PRODUCED BY
COLLAPSE OF A SPHERICAL CAVITY

by

R. S. BRAND

MECHANICAL ENGINEERING DEPARTMENT

This research was carried out under the
Bureau of Ships Fundamental Hydromechanics
Research Program S-RO09 01 01, administered
by the David Taylor Model Basin

Contract Nonr 3292 (01)

STORRS, CONNECTICUT

JUNE, 1962

This uniform plan of publishing technical reports for the School of Engineering of the University of Connecticut was inaugurated in June, 1962. Copies of reports can be obtained by writing to:

Office of the Dean
School of Engineering
University of Connecticut
Storrs, Connecticut

Reproduction in whole or in part is
permitted for any purpose of the
United States Government

The Shock Wave Produced by Collapse
of a Spherical Cavity

by

R. S. Brand

ABSTRACT

The results of the computations for a single case of spherical cavity collapse in water are presented, including the post-collapse shock wave and accompanying velocity and pressure fields. For the model studied it appears that at a finite time after collapse negative pressures occur, indicating that the cavity reopens.

TABLE OF CONTENTS

	PAGE
Abstract	ii
Purpose and Scope	1
List of Symbols	3
Theory	4
Results	8
Acknowledgements	17
References	17
Appendix -- Details of the Computations	
A. Characteristics	18
B. The Shock Wave	19
C. Points on the Cavity Boundary	22
D. Points on the Solid Boundary	23
Distribution List	26

The Shock Wave Produced by Collapse
of a Spherical Cavity

PURPOSE AND SCOPE

This investigation is concerned with the pressure and velocity fields which surround an empty cavity collapsing with spherical symmetry in water.

It is assumed that the cavity suddenly appears in an infinite expanse of water which is at rest and at uniform pressure, p_∞ . Since all lengths are made dimensionless with respect to the initial cavity radius, the only parameter which affects the collapse is p_∞ . In this report only a single case is presented, that for which $p_\infty / B = 0.02$. B is a constant appearing in the equation of state; for water it is approximately 3 kilobars.

The water is assumed to be inviscid and compressible.

The discontinuity in pressure at the cavity boundary (zero pressure in the cavity, p_∞ just outside) cannot persist. An expansion wave moves outward, and behind this wave the fluid and the cavity wall move inward. The method of characteristics is used to compute this motion.

Since the numerical solution cannot be carried to zero radius, it is assumed that the cavity collapses on a small solid sphere. In the case reported here the ratio of the radius of this sphere to the initial cavity is .00423. When the inrushing water strikes this small rigid sphere, its motion is arrested by a spherical shock wave moving outward. It is the major object of this investigation to describe this shock wave. It is speculated that the properties of the shock do not depend strongly on the size of the solid sphere once the shock has moved a small distance away.

In fact, it is hoped that the present results are at least qualitatively descriptive of the shock that would be produced by an absolutely empty cavity.

Calculation of the shock is carried to a time when the radius of the shock is almost twice the initial cavity radius. By this time the velocity of the shock is nearly sonic and the pressure ratio across it is nearly one. That is, it has, within the limits of accuracy of the numerical work, degenerated into a continuous wave.

The flow behind the shock is also computed by the method of characteristics. It is found that at the solid sphere the pressure eventually falls to zero indicating that the cavity reopens. Indeed, a sequence of several openings and closings is indicated by the calculations. However, since the principal purpose was to compute the shock, the behavior at the solid boundary has not been adequately investigated.

LIST OF SYMBOLS

B	constant appearing in the equation of state
c	speed of sound
c_0	speed of sound corresponding to zero pressure
$C=c/c_0$	dimensionless speed of sound
c_{r0}	speed of sound in undisturbed water
C_A	dimensionless speed of sound just outside shock
C_B	dimensionless speed of sound just inside shock
p	pressure
$P=p/B$	dimensionless pressure
P_{r0}	dimensionless pressure in undisturbed water
r	radial distance from center of cavity
r_0	initial cavity radius
$R=r/r_0$	dimensionless radial co-ordinate
R_{min}	dimensionless radius of solid sphere
t	time
$T=c_0 t/r_0$	dimensionless time
u	velocity of fluid
$U=u/c_0$	dimensionless velocity of fluid
w	velocity of shock wave
$W=w/c_0$	dimensionless velocity of shock wave
γ	exponent in equation of state
ρ	density
ρ_0	density corresponding to zero pressure

THEORY

It is assumed that at time $t=0$ an empty spherical cavity of radius r_0 suddenly appears in an infinite expanse of water which is at rest and at some uniform pressure p_∞ .

The water is taken to be a compressible fluid having an equation of state

$$\frac{p}{B} = \left(\frac{\rho}{\rho_0} \right)^\gamma - 1 \quad (1)$$

where ρ is the density corresponding to pressure p , ρ_0 is the non-zero density corresponding to zero pressure, and B and γ are constants characteristic of the liquid. For water B is approximately 3 kilobars and γ is approximately 7.

The speed of sound, c , can be computed from (1) as

$$c^2 = \frac{B\gamma}{\rho_c} \left(\frac{\rho}{\rho_0} \right)^{\gamma-1} = c_0^2 \left(\frac{\rho}{\rho_c} \right)^{\gamma-1} \quad (2)$$

where c_0 is the sound speed that would prevail in water at zero pressure.

Hence (1) can be written

$$p/B = (c/c_0)^{2\gamma/(\gamma-1)} - 1 \quad (3)$$

or

$$P = C \frac{2\gamma}{\gamma-1} - 1$$

in which $P = p/B$ and $C = c/c_0$.

The dimensionless sound speed, C , is the most convenient thermodynamic state variable, and all results are given in terms of C . The pressure is easily computed from C by means of equation (3).

It is apparent that relatively small changes in C denote very high pressures. For example $C = 1.03$ corresponds approximately to $P = 1.07$ or $p = 210$ bars. (Recall that $C = 1.00$ corresponds to $p = 0$.) In some parts of the computations values of C of 50 and greater were obtained. It is doubtful that the assumed equation of state is valid for such conditions.

The problem is to determine u , the fluid velocity and c , the sound speed as functions of r , the distance from the center of the cavity, and t , the time measured from the start of the collapse. These variables are made dimensionless by choosing c_0 as a reference velocity and r_0 , the initial cavity radius, as a length scale.

$$R = r/r_0 \quad T = c_0 t/r_0 \quad U = u/c_0 \quad C = c/c_0 \quad (4)$$

In terms of these variables the differential equations expressing the conservation of mass and of momentum can be combined to form a pair of simultaneous first order partial differential equations in which, in each equation, the dependent variables U and C are differentiated in the same direction in the R - T plane.

$$\frac{\partial U}{\partial T} + (U + C) \frac{\partial U}{\partial R} + \frac{2}{\gamma - 1} \left[\frac{\partial C}{\partial T} + (U + C) \frac{\partial C}{\partial R} \right] = -2 \frac{UC}{R} \quad (5)$$

$$\frac{\partial U}{\partial T} + (U - C) \frac{\partial U}{\partial R} - \frac{2}{\gamma - 1} \left[\frac{\partial C}{\partial T} + (U - C) \frac{\partial C}{\partial R} \right] = 2 \frac{UC}{R} \quad (6)$$

The family of lines for which $\frac{dR}{dT} = U + C$ are called outgoing characteristics. It follows from equation (5) that for a differential increment along such a line

$$dR = (U + C) dT$$

$$dU + \frac{2}{\gamma - 1} dC = \frac{-2UC}{R} dT \quad (7)$$

while for an ingoing characteristic for which $\frac{dR}{dT} = U - C$, we have from (6)

$$\begin{aligned} dR &= (U - C) dT \\ dU - \frac{2}{\gamma-1} dC &= \frac{2UC}{R} dT \end{aligned} \quad (8)$$

The computations reported here are based on finite difference approximations to equations (7) and (8).

It is of course not possible to carry the computations all the way to $R = 0$ because of the $\frac{1}{R}$ factors occurring on the right hand sides of (7) and (8). Accordingly the expedient was adopted of assuming that at the center of the cavity there exists a small solid sphere of (dimensionless) radius R_{\min} . R_{\min} was not chosen at the outset but was taken to be the smallest positive value of R which could be reached by reducing the mesh size of the characteristic network a pre-selected number of times. In the case reported here $R_{\min} = 0.00423$.

When the intruding cavity boundary strikes this solid sphere, its motion is arrested instantly. This discontinuity in the fluid velocity is the origin of a shock wave which moves outward very rapidly at first but with decreasing velocity. The shock wave is treated here as a true mathematical discontinuity; that is, at the shock at each instant there are two values of U and two of C . These are related to each other and to W the dimensionless shock velocity by

$$\frac{U_B - W}{U_A - W} = \left(\frac{C_A}{C_B} \right)^{\frac{2}{\gamma-1}} \quad (9)$$

$$(U_B - W)(U_A - U_B) = \frac{1}{\gamma} C_B^2 \left[1 - \left(\frac{C_A}{C_B} \right)^{\frac{2\gamma}{\gamma-1}} \right] \quad (10)$$

in which subscript "A" refers to the fluid just ahead (i.e. outside) the shock and subscript "B" refers to the fluid inside the shock.

Equations (9) and (10) are derived from the statements of conservation of mass and momentum together with the assumption that the equation of state (1) holds across the shock, an assumption justified by the fact that the state of water is quite insensitive to entropy. Hence the mechanical conditions are sufficient to describe the shock process and no consideration need be given to the energy equation. (See reference 1, pp. 131-132)

Solutions to equations (9) and (10) must be obtained at every point on the shock which are compatible with the characteristic equations on both sides. A more detailed description of how this was done is given in the Appendix.

The boundary conditions for the problem are as follows:

- (1) On $R = T + 1$, which is the leading edge of the outgoing expansion wave which originates at $R = 1.0$, $T = 0$, we have $P = P_\infty$ or $C = C_\infty$.
- (2) During the collapse phase on the cavity boundary, which is an undetermined curve in the R - T plane, $C = 1$
- (3) After collapse, when $R = R_{\min}$, $U = 0$

It was found that in applying boundary condition (3), values of $C < 1.0$ were encountered. This would imply that the cavity was reopened. When this occurred, the values obtained were rejected and boundary condition (2) was substituted for (3).

Several cycles of opening and closing were obtained but the size of the finite steps taken was such that this behavior is not well delineated.

RESULTS

The results of the computations are shown in the curves, Figs. (1) through (8).

Fig. (1) shows the cavity wall path, the shock, and several representative characteristics. Figs. (2) and (3) are enlargements near the collapse point of the same information. It should be pointed out that even in Fig. (3), which shows considerable detail near $R = R_{\min}$, only a fraction of the characteristics actually computed have been plotted.

Fig. (4) is a log-log plot of the velocity of the cavity boundary vs. the cavity radius. From the slope of this curve, which is nearly a straight line for small R , it can be determined that the final collapse appears to follow a law of the type.

$$\dot{R} = - R^{\alpha}$$

with $\alpha = -0.90$. This tends to confirm Hunter's analysis (Reference 2)

Figs. (5) and (6) are descriptive of the shock, showing its velocity and strength (i.e. the sound speed on both sides of the shock) plotted against the radius of the shock.

Figs. (7) and (8) show the variation of sound speed with radius at different times, and is thus descriptive of the pressure field.

All of the results given in the curves are for $P_{\infty} = p_{\infty}/B = 0.02$ and $R_{\min} = 0.00423$

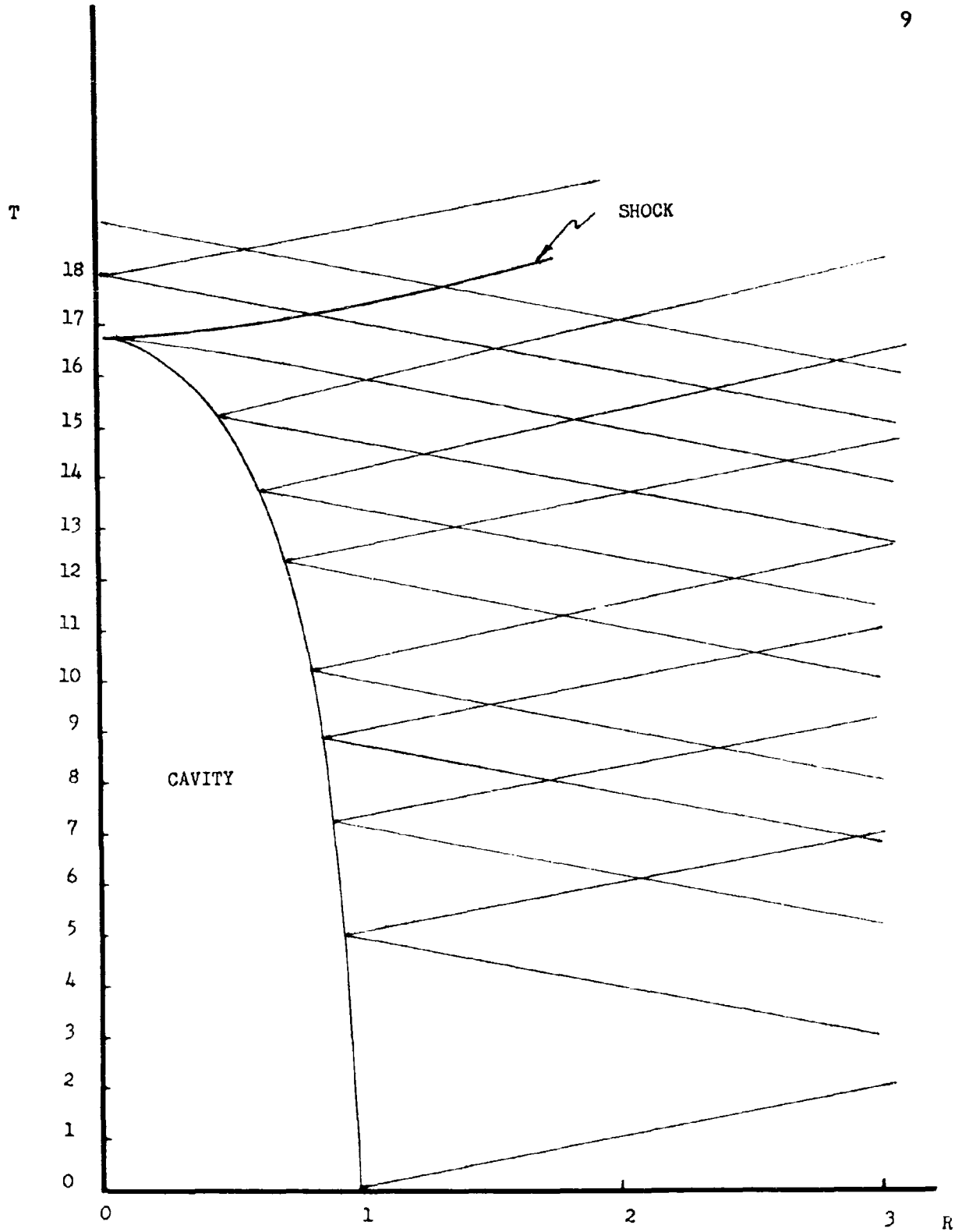


FIGURE 1.

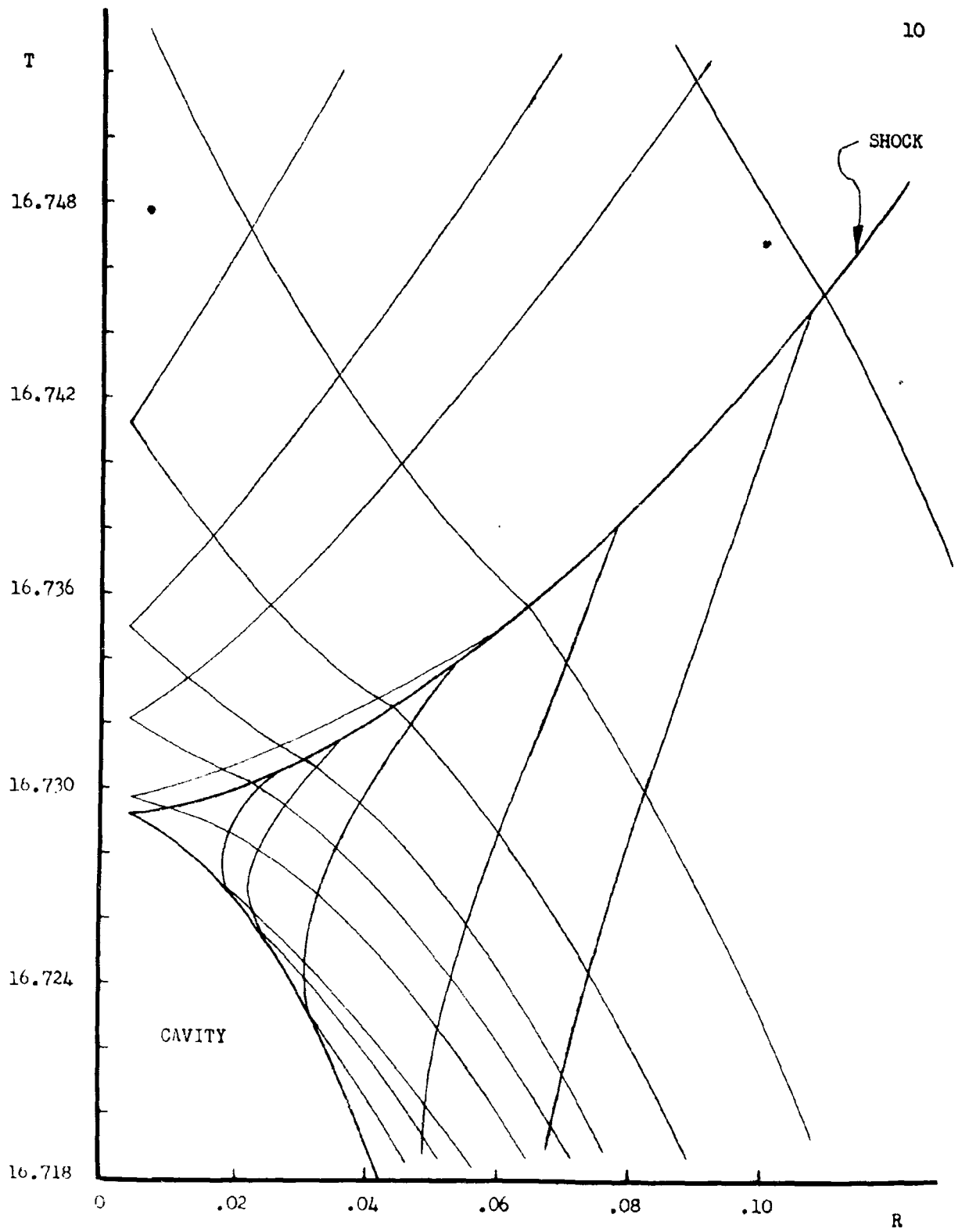


FIGURE 2.

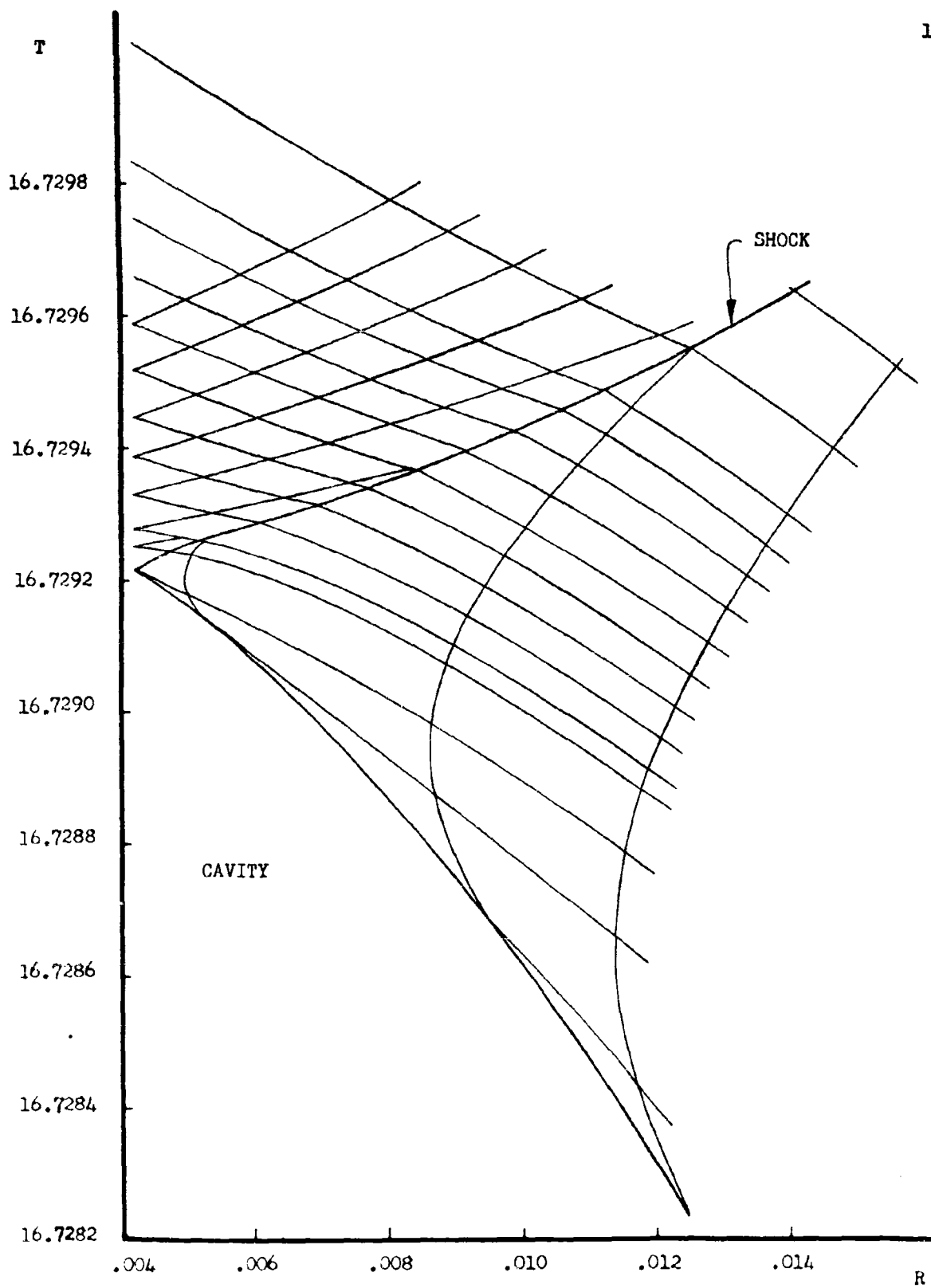


FIGURE 3.

CAVITY WALL VELOCITY VS. CAVITY RADIUS

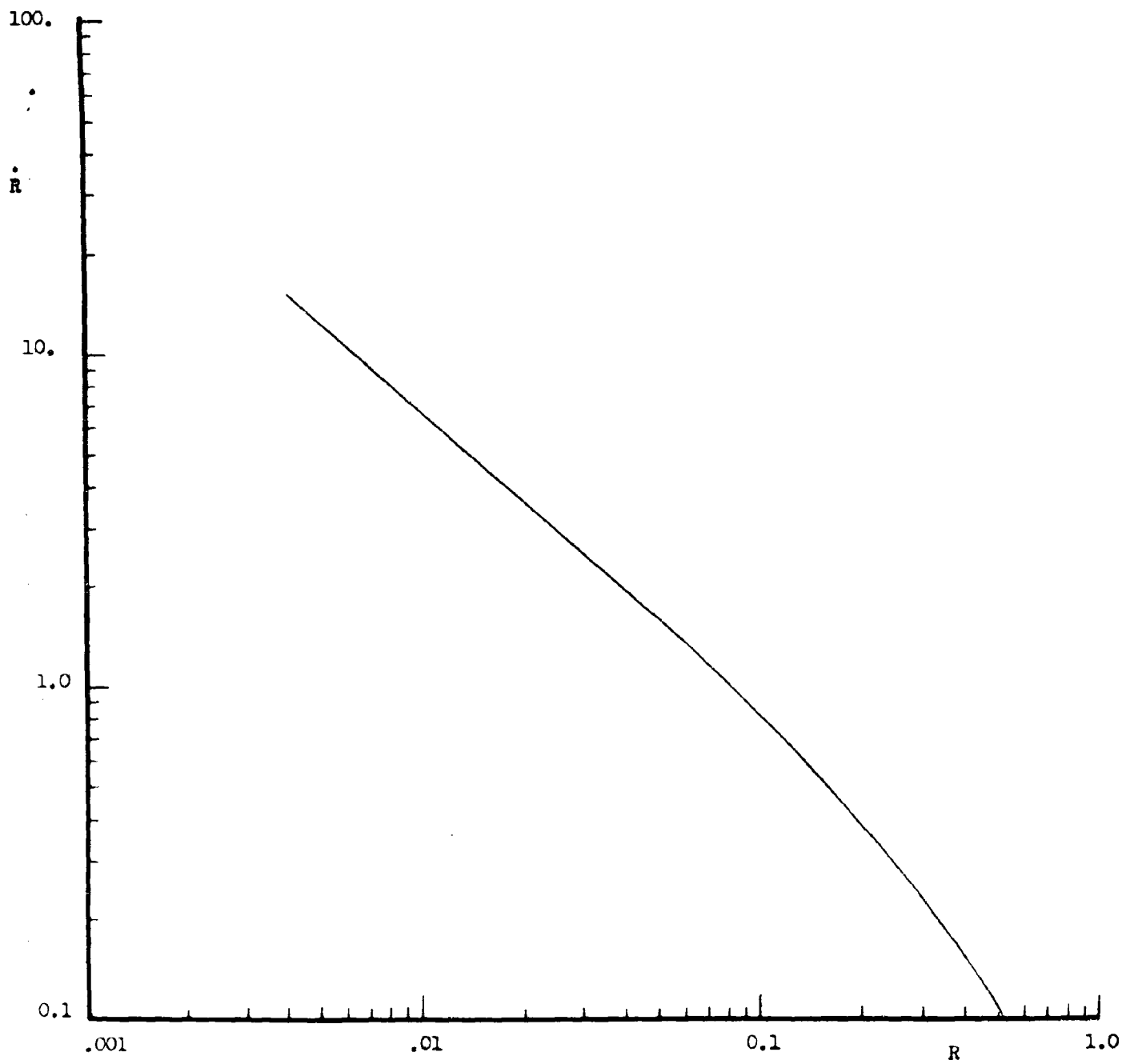


FIGURE 4

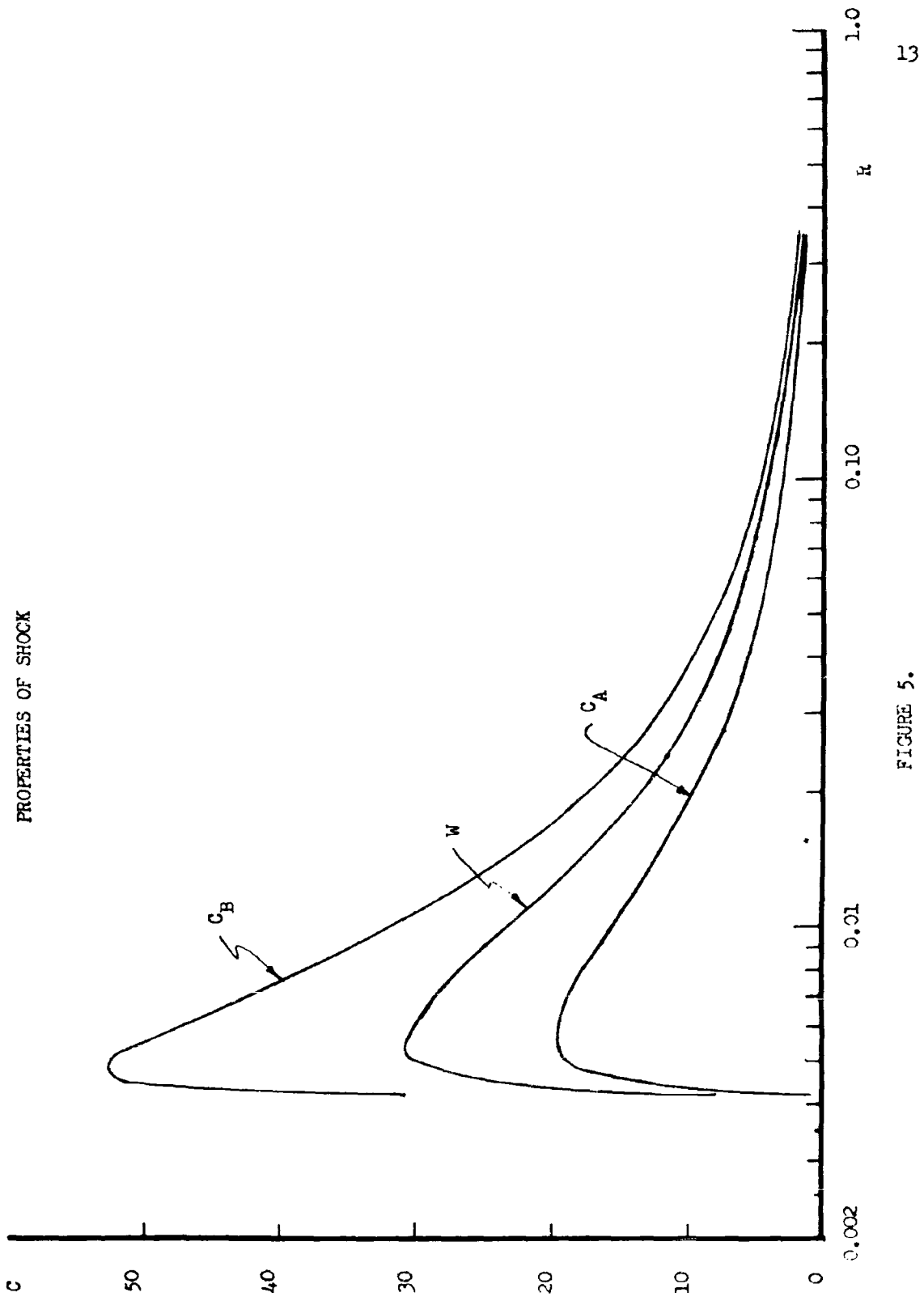


FIGURE 5.

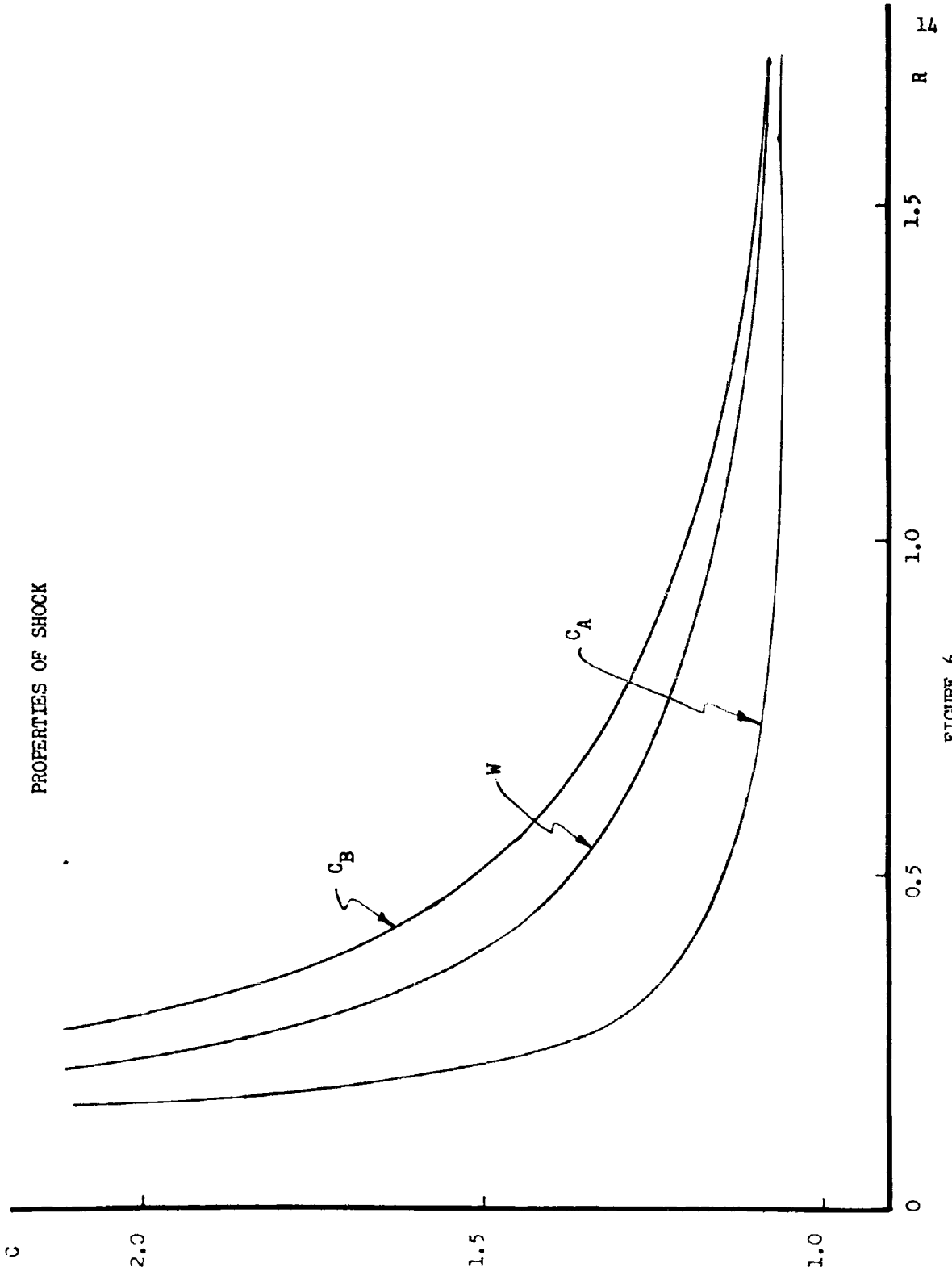


FIGURE 6.

SOUND SPEED VS. RADIUS
AT CONSTANT TIME
(BEFORE SHOCK OCCURS)

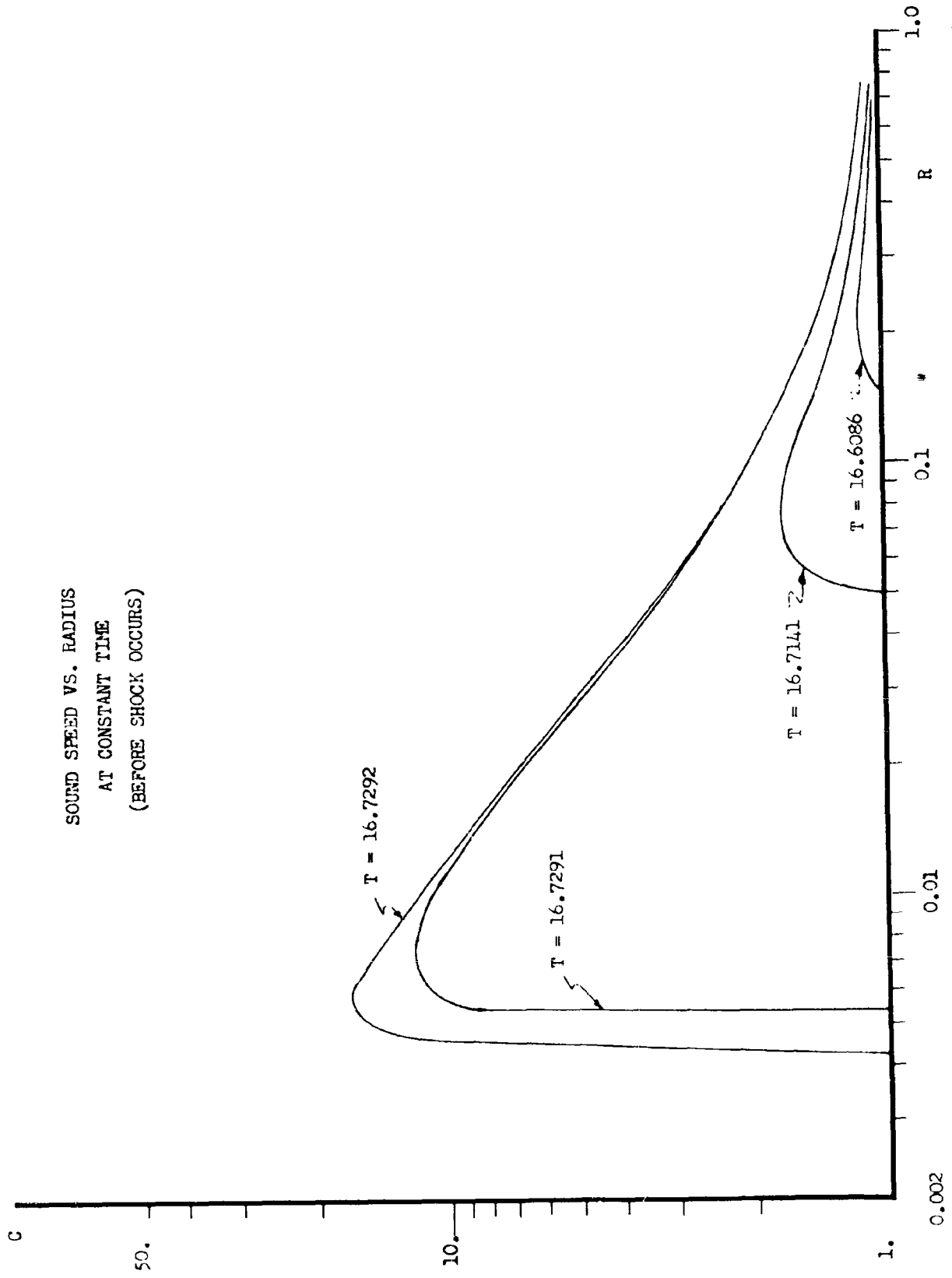


FIGURE 7.

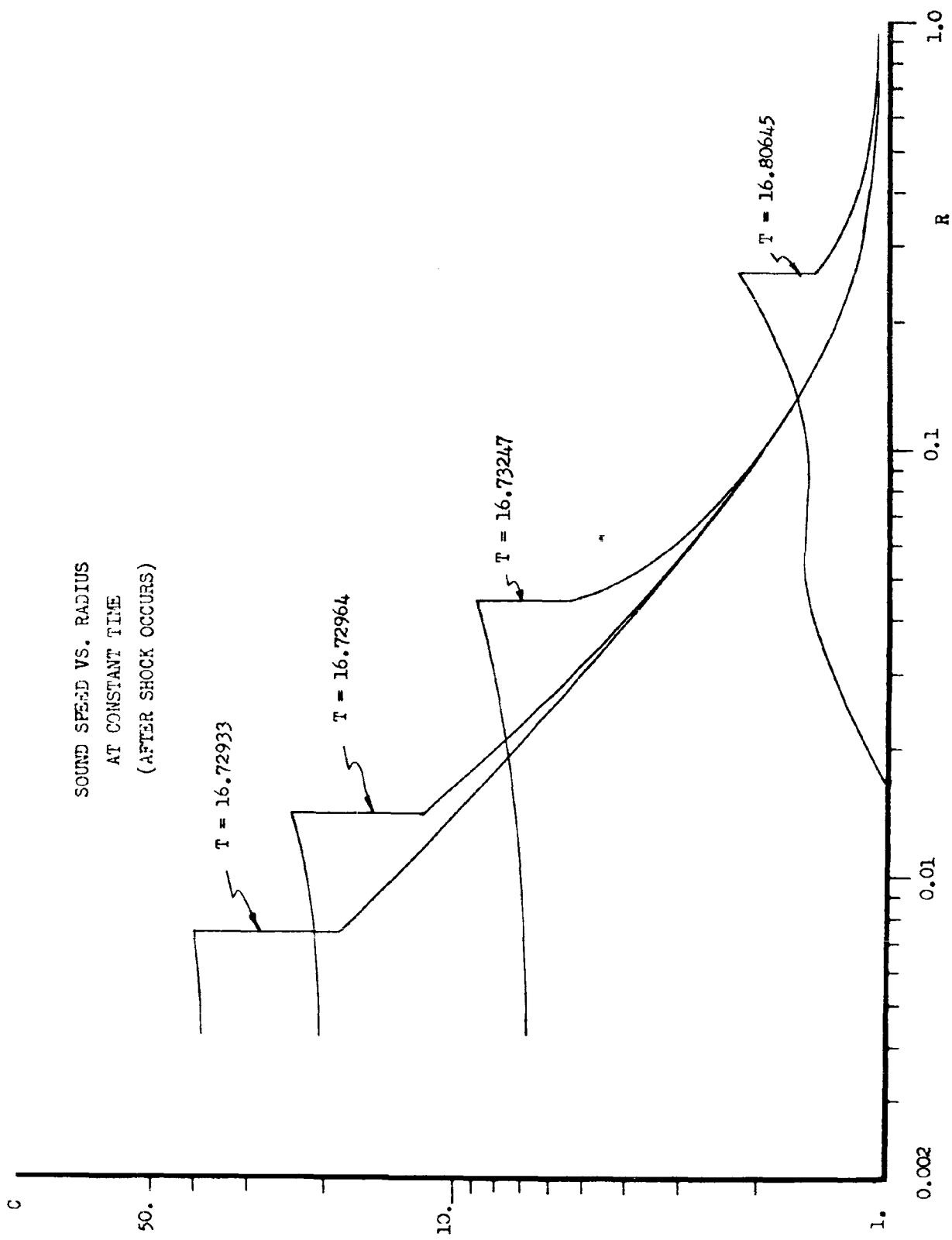


FIGURE 8.

ACKNOWLEDGEMENTS

Mr. Paul Nemerlut, Research Assistant, and Mr. Mario Casarella, Instructor in Mechanical Engineering, assisted in carrying out the computations.

Computations were performed on the IBM 7090 Computer at the Massachusetts Institute of Technology Computation Center, Cambridge, Massachusetts.

REFERENCES

1. Courant, R. and Friedrichs, K. O.; Supersonic Flow and Shock Waves, Interscience Publishers, N. Y., 1948
2. Hunter, C.; "On the Collapse of an Empty Cavity in Water"; Journal of Fluid Mechanics, vol. 8, part 2, p. 241-263; June, 1960

APPENDIX

Details of the Computations

A. Characteristics

Computation proceeded stepwise along the ingoing characteristics. Assume that, in Fig. (9), values of R , T , U , and C , have been found at all the mesh points indicated by the solid lines, including points 1 and 2, and we now wish to compute R_3 , T_3 , U_3 , and C_3 .

The finite difference approximations to (7) and (8) are

$$R_3 - R_1 = \frac{1}{2}(U_1 + C_1 + U_3 + C_3) (T_3 - T_1) \quad (11)$$

$$U_3 - U_1 + \frac{2}{\gamma-1} (C_3 - C_1) = - \left(\frac{U_1 C_1}{R_1} + \frac{U_3 C_3}{R_3} \right) (T_3 - T_1) \quad (12)$$

$$R_3 - R_2 = \frac{1}{2}(U_2 - C_2 + U_3 - C_3) (T_3 - T_2) \quad (13)$$

$$U_3 - U_2 - \frac{2}{\gamma-1} (C_3 - C_2) = \left(\frac{U_2 C_2}{R_2} + \frac{U_3 C_3}{R_3} \right) (T_3 - T_2) \quad (14)$$

The simultaneous solution of these four non-linear equations was effected by an iterative process on the equations

$$R_3 - R_1 = K_1 (T_3 - T_1) \quad (15)$$

$$U_3 - U_1 + \frac{2}{\gamma-1} (C_3 - C_1) = - K_2 (T_3 - T_1) \quad (16)$$

$$R_3 - R_2 = K_3 (T_3 - T_2) \quad (17)$$

$$U_3 - U_2 - \frac{2}{\gamma-1} (C_3 - C_2) = K_4 (T_3 - T_2) \quad (18)$$

Initially the coefficients K_i were approximated by

$$K_1 = U_1 + C_1 \quad K_2 = 2 \frac{U_1 C_1}{R_1} \quad K_3 = U_2 - C_2 \quad K_4 = 2 \frac{U_2 C_2}{R_2}$$

all of which are known. Equations (15) through (18) are then linear and

are easily solved for R_3 , T_3 , U_3 , C_3 . New values of the coefficients K_i are then computed from

$$K_1 = \frac{1}{2}(U_1 + C_1 + U_3 + C_3) \quad K_2 = \frac{U_1 C_1}{R_1} + \frac{U_3 C_3}{R_3}$$

$$K_3 = \frac{1}{2}(U_2 - C_2 + U_3 - C_3) \quad K_4 = \frac{U_2 C_2}{R_2} + \frac{U_3 C_3}{R_3}$$

Use of these improved values of the K_i in equations (15) through (18) lead to improved values of R_3 , T_3 , U_3 , C_3 . The process is repeated until the change in R_3 from one iteration to the next is less than a pre-selected tolerance.

B. The Shock Wave

Let it be assumed that calculations have been completed on the characteristic labelled "100" in Fig. (10), including all values at the shock. Calculations on characteristic "101" have been carried up to and including point 4, and we now wish to compute the location of and flow parameters at point 5. That is, the values of R , T , U , and C are known at points 1, 3, and 4, and at 2 we have R , T , U_A , C_A , U_B , C_B , and W . We now wish to calculate the seven unknowns associated with the shock at point 5.

Point 5 is at the intersection of the shock wave with the ingoing characteristic "101". Because a shock wave always has a supersonic velocity relative to the fluid ahead of it, there must be an outgoing characteristic arising from some point on characteristic "100" between points 1 and 2, which also passes through point 5. This auxiliary point is labelled 7 in the diagram and the auxiliary characteristic is shown as a dashed line.

Similarly, behind the shock, there must be a point 8, between 2 and

3, where an outgoing characteristic will also intersect the shock at point 5, because a shock always has a subsonic speed relative to the fluid behind it.

It is assumed that the parameters at point 7 are related by a linear interpolation between points 1 and 2, and that 8 is similarly related to 2 and 3.

We now summarize the unknowns and the available equations.

Unknowns:

At point 5 - $R_5, T_5, U_{A-5}, C_{A-5}, U_{B-5}, C_{B-5}, W_5$

At point 7 - R_7, T_7, U_7, C_7

At point 8 - R_8, T_8, U_8, C_8

Equations

Shock relations (9) and (10) at point 5 (2 equations)

Characteristic equations relating $R_5, T_5, U_{A-5}, C_{A-5}$ to points 4 and 7. (4 equations)

Characteristic equations for outgoing characteristic only, relating $R_5, T_5, U_{B-5}, C_{B-5}$ to R_8, T_8, U_8, C_8 (2 equations)

Interpolation for point 7 between 1 and 2 (3 equations)

Interpolation for point 8 between 2 and 3 (3 equations)

Velocity of the shock

$$(R_5 - R_2) / (T_5 - T_2) = \frac{1}{2}(W_5 + W_2) \quad (1 \text{ equation})$$

Thus we have 15 relationships available for determining the 15 unknowns.

The sequence adopted for solving these equations was as follows:

1. Assume a value of W_5 (The initial assumption was $W_5 = W_2$)
2. Assume a value of R_7 . (Initial choice: $R_7 = \frac{1}{2}(R_1 + R_2)$)
3. Find T_7, U_7 , and C_7 by interpolation between 1 and 2.

4. Using points 4 and 7 as input, find R_5 , T_5 , U_{A-5} , C_{A-5} , by means of the characteristics subroutine.

5. Test whether the point R_5 , T_5 determined in step 4 lies on the shock;

$$(R_5 - R_2) / (T_5 - T_2) = \frac{1}{2}(W_2 + W_5) ?$$

If this relation is not satisfied closely enough, adjust the value of R_7 and return to step 3.

If the relation is satisfied, proceed to step 6.

6. Since we now have values of U_{A-5} , C_{A-5} and W_5 , the shock relations have only two unknowns, U_{B-5} and C_{B-5} . Solve these simultaneously. (A Newton-Raphson iteration was used, rather than simple elimination of one of the unknowns because of the complexity of the equations.)

7. Assume a value of R_8 (Initial choice: $R_8 = \frac{1}{2}(R_2 + R_3)$)

8. Interpolate for T_8 , U_8 , and C_8 , between points 2 and 3

9. Test whether the point R_5 , T_5 , lies on the outgoing characteristic through point 8;

$$(R_5 - R_8) / (T_5 - T_8) = \frac{1}{2}(U_8 + C_8 + U_{B-5} + C_{B-5}) ?$$

If this test is not met within the specified tolerance, adjust R_8 and return to step 8.

If the test is met, proceed to step 10.

10. Compare the value of U_{B-5} determined by the shock in step 6 with the value of U_{B-5} that the characteristic relation for an outgoing characteristic would predict. Let the difference between these values of U_{B-5} be an error E

$$E = U_{B-5} (\text{shock}) - U_8 + \frac{2}{\gamma-1} (C_{B-5} - C_8) - \left(\frac{U_{B-5} C_{B-5}}{R_5} + \frac{U_8 C_8}{R_1} \right) (T_5 - T_8)$$

11. Assume a new value of W_5 somewhat less than W_2 and repeat the entire process of steps 2 through 10, finding a new value of E corresponding to the new value of W_5
12. Assuming a linear relationship between E and W_5 , make a third choice of W_5 which will reduce E to zero.
13. Continue until the $(n + 1)^{\text{th}}$ choice of W_5 differs from the n^{th} choice by less than a pre-assigned tolerance.

C. Points on the Cavity Boundary

On the boundary of the collapsing cavity the pressure is zero and hence $C = 1$. The velocity of the liquid is the velocity of the boundary itself.

In Fig. 11, let us assume that the calculations for ingoing characteristic "50" are complete (including the boundary point, 1), and that on characteristic "51" we have computed up to and including point 2 by the method of characteristics as described in Section A above. We now wish to establish boundary point 3 on characteristic "51".

Unknowns are R_3 , T_3 , U_3 . C_3 is known to be unity because of the condition of zero pressure in the cavity.

The fact that both points 1 and 3 are on the cavity boundary where the velocity of the boundary is the velocity of the fluid is expressed by

$$(R_3 - R_1) / (T_3 - T_1) = \frac{1}{2}(U_1 + U_3) \quad (19)$$

Since both 3 and 2 are on the same ingoing characteristic, relations (13) and (14) apply

$$R_3 - R_2 = \frac{1}{2}(U_2 - C_2 + U_3 - C_3) (T_3 - T_2) \quad (20)$$

$$U_3 - U_2 - \frac{2}{\gamma - 1} (C_3 - C_2) = \left(\frac{U_2 C_2}{R_2} + \frac{U_3 C_3}{R_3} \right) (T_3 - T_2) \quad (21)$$

Equations (19), (20) and (21) are sufficient to determine R_3 , T_3 , and U_3 . Actual solution of the equations was carried out by an iterative

technique very similar to that employed in the method of characteristics for points not on the boundary.

D. Points on the Solid Boundary

The calculations are based on the assumption that the cavity collapses onto a rigid sphere of radius R_{\min} . Hence the ingoing characteristics which cross the shock are terminated at that radius, and in Fig. 12 it is necessary to compute point 2 from point 1, using $R_2 = R_{\min}$, $U_2 = 0$; with C_2 and T_2 determined by the ingoing characteristic equations:

$$R_2 - R_1 = \frac{1}{2}(U_2 - C_2 + U_1 - C_1) (T_2 - T_1)$$

$$U_2 - U_1 - \frac{2}{\gamma-1} (C_2 - C_1) = \left(\frac{U_2 C_2}{R_2} + \frac{U_1 C_1}{R_1} \right) (T_2 - T_1)$$

Simultaneous solution of these equations for C_2 and T_2 is routine.

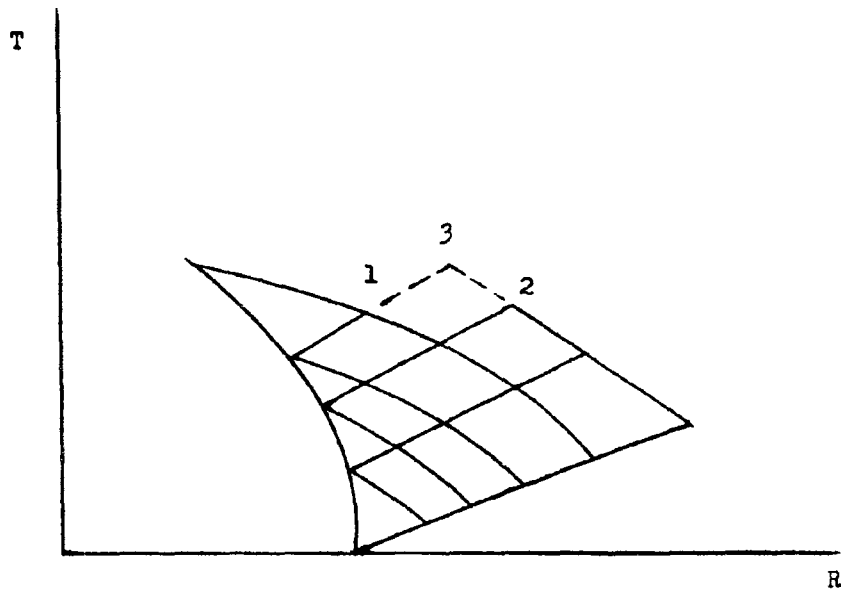


FIGURE 9

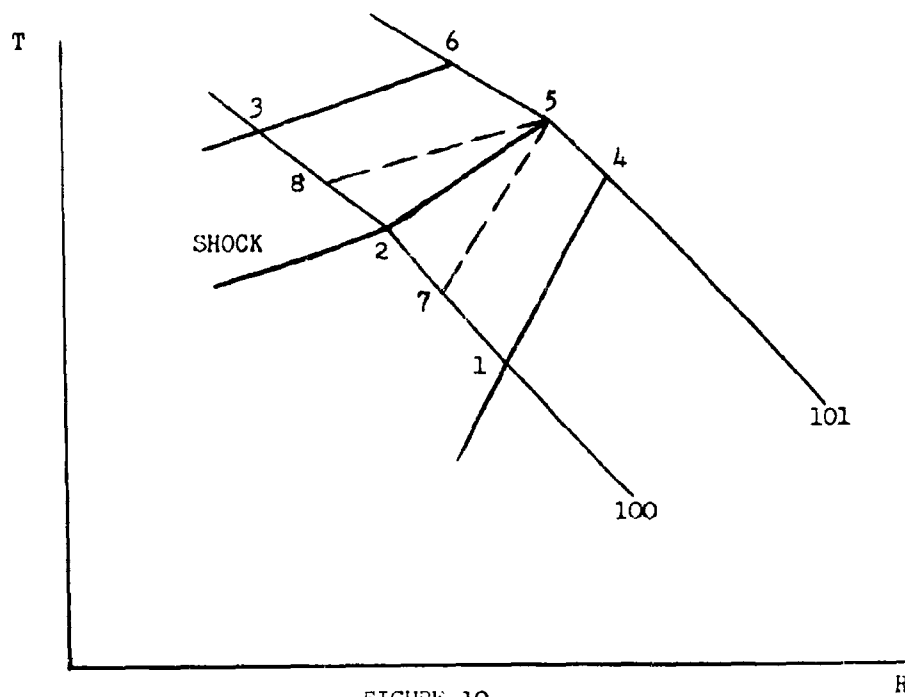


FIGURE 10

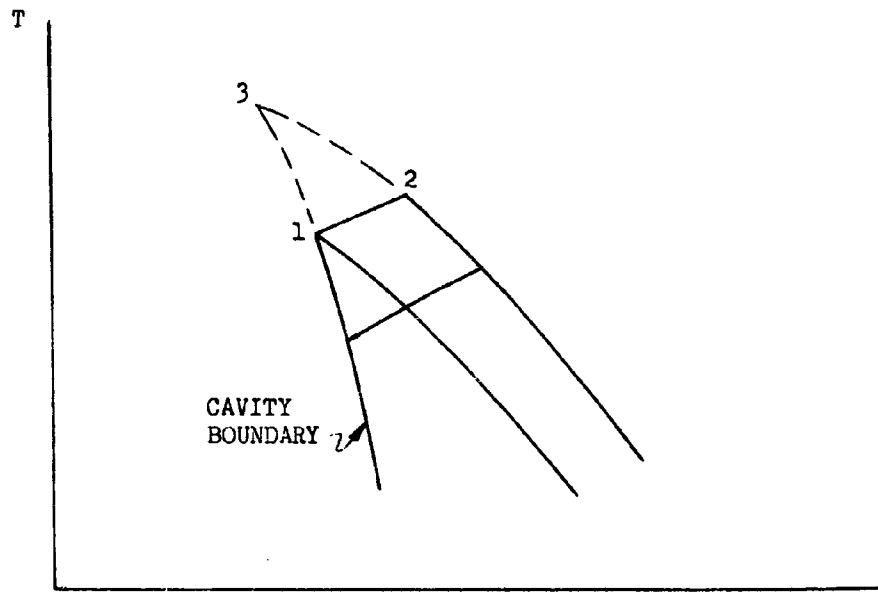


FIGURE 11.

R

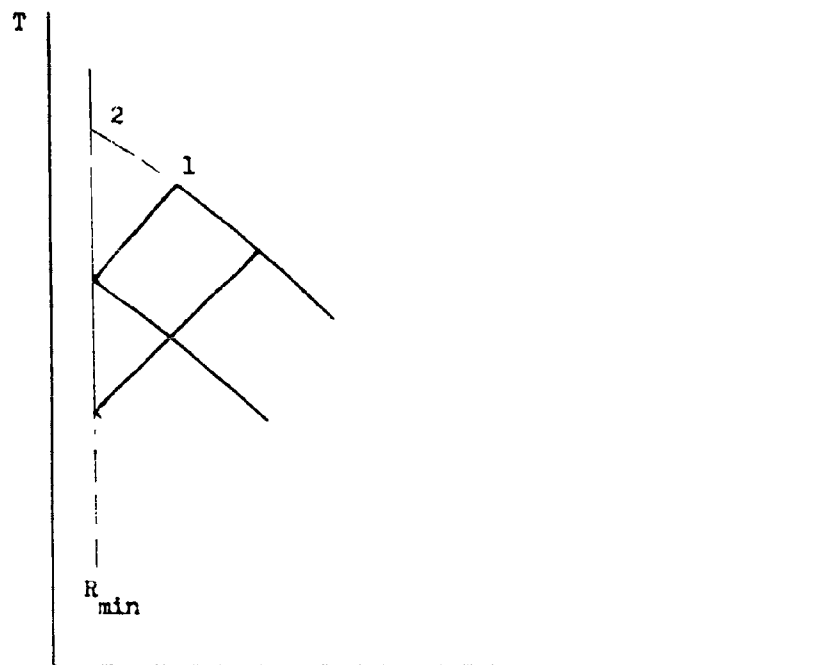


FIGURE 12.

R

DISTRIBUTION LIST

Copies		Copies	
75	David Taylor Model Basin Washington 7, D. C. Attn: Contract Research - Code 513	2	Director, Naval Research Laboratory Washington 25, D. C. Attn: Code 2021
7	Chief, Bureau of Ships Department of the Navy Washington 25, D. C. Attn: (1) Technical Information - Code 335 (1) Ship Silencing - Code 341B (1) Ship Design - Code 410 (1) Preliminary Design - Code 420 (1) Hull Design - Code 440 (1) Laboratory Management - Code 320	2	Commander Naval Ordnance Laboratory, White Oak Silver Spring, Maryland Attn: Library
		2	National Aeronautics and Space Administration 1512 H Street, N. W. Washington 25, D. C.
		10	Astia Document Service Center Arlington Hall Station Arlington 12, Virginia
1	Commanding Officer Office of Naval Research Branch Office 493 Summer Street Boston 10, Massachusetts	1	Society of Naval Architects and Marine Engineers 74 Trinity Place New York 6, New York Attn: Librarian
1	Commanding Officer Office of Naval Research Branch Office 207 West 24th Street New York 11, New York	1	U.S. Naval Boiler and Turbine Laboratory Naval Base Philadelphia 12, Pennsylvania
1	Commanding Officer Office of Naval Research Branch Office The John Crerar Library Building 86 East Randolph Street Chicago 1, Illinois	1	U. S. Naval Underwater Sound Laboratory New London, Connecticut
1	Commanding Officer Office of Naval Research Branch Office 1000 Geary Street San Francisco 9, California	1	National Bureau of Standards National Hydraulics Laboratory Washington 25, D. C.
1	Commanding Officer Office of Naval Research Branch Office 1030 East Green Street Pasadena, California	1	Accurate Products Company 400 Hillside Avenue Hillside, New Jersey
		2	Brown University Providence, Rhode Island Attn: (1) Division of Applied Mathematics (1) Professor W. H. Reid

Copies

2 California Institute of Technology
Pasadena 4, California
Attn: (1) Hydrodynamics Laboratory
(1) Dr. A. T. Ellis

2 University of California
Berkeley 4, California
Attn: (1) College of Engineering
(1) Professor Maurice Holt

1 Carnegie Institute of Technology
Pittsburgh 13, Pennsylvania

1 Colorado State University
Hydraulics Laboratory
Fort Collins, Colorado

1 University of Colorado
Hydraulic Laboratory
Boulder, Colorado

1 Cornell University
School of Civil Engineering
Applied Hydraulic Laboratory
Ithaca, New York

1 University of Delaware
Fluids Laboratory
Newark, Delaware

1 Douglas Aircraft Company
El Segundo Division
827 Lapham Street
El Segundo, California

1 University of Florida
Engineering and Industrial
Experiment Station
Gainesville, Florida

1 Georgia Institute of Technology
Hydraulics Laboratory
Atlanta, Georgia

1 General Dynamics Corporation
Electric Boat Division -
Applied Mechanics Section
Groton, Connecticut

Copies

1 Harvard University
Acoustics Laboratory
Cambridge, Massachusetts

1 Hydronautics, Incorporated
200 Monroe Street
Rockville, Maryland

1 Illinois Institute of Technology
Applied Mechanics Department
Chicago, Illinois

1 University of Illinois
Department of Theoretical and
Applied Mechanics
Urbana, Illinois

1 Iowa Institute of Hydraulic Research
State University of Iowa
Iowa City, Iowa

1 Johns Hopkins University
Applied Physics Laboratory
Silver Spring, Maryland

1 Johns Hopkins University
School of Engineering
Baltimore 18, Maryland

1 University of Kansas
Department of Engineering Mechanics
Lawrence, Kansas

1 Lehigh University
Bethlehem, Pennsylvania

1 University of Maryland
Institute for Fluid Dynamics and
Applied Mathematics
College Park, Maryland

1 Massachusetts Institute of
Technology
Computation Center
Cambridge, Massachusetts

1 Massachusetts Institute of
Technology
Department of Civil Engineering
Cambridge, Massachusetts

Copies

1 University of Michigan
Engineering Mechanics Department
Ann Arbor, Michigan

1 University of Minnesota
School of Engineering
Minneapolis, Minnesota

1 University of Nebraska
Department of Engineering Mechanics
Lincoln, Nebraska

1 New York University
College of Engineering
New York 53, New York

1 North Carolina State College
Department of Engineering Research
Raleigh, North Carolina

1 Northwestern University
The Technological Institute
Evanston, Illinois

1 University of Notre Dame
School of Engineering
Notre Dame, Indiana

1 Pennsylvania State University
Ordnance Research Laboratory
University Park, Pennsylvania

1 Purdue University
School of Mechanical Engineering
Lafayette, Indiana

1 Reed Research Foundation
1048 Potomac Street, N. W.
Washington 7, D. C.

1 Republic Aviation Corp.
Farmingdale, Long Island, N. Y.
Attn: Mr. D. D. Duclos
Plasma Propulsion Project

1 University of Rhode Island
Mechanical Engineering Department
Kingston, Rhode Island

Copies

1 R.P.I. Graduate Center
South Windsor, Connecticut
Attn: Professor H. W. Butler

1 Scripps Institution of Oceanography
La Jolla, California

1 Southwest Research Institute
San Antonio 6, Texas

1 Stanford University
Hydraulic Laboratory
Stanford, California

1 Stevens Institute of Technology
Davidson Laboratory
Hoboken, New Jersey

1 Robert Taggart Incorporated
400 Arlington Boulevard
Falls Church, Virginia

1 University of Tennessee
Knoxville 16, Tennessee

1 Texas A and M College
College Station, Texas

1 University of Texas
Austin 12, Texas

1 Washington State University
Pullman, Washington

1 University of Washington
Seattle 5, Washington

1 University of Wisconsin
Madison, Wisconsin

1 Woods Hole Oceanographic Institution
Woods Hole, Massachusetts

1 Worcester Polytechnic Institute
Alden Hydraulic Laboratory
Worcester 9, Massachusetts